Dynamical Effects of the Martensitic Transition in Magnetocaloric Heusler Alloys from Direct ΔT_{ad} Measurements under Different Magnetic-Field-Sweep Rates

T. Gottschall,[1,*] K. P. Skokov,[1] F. Scheibel,[2] M. Acet,[2] M. Ghorbani Zavareh,[3,4] Y. Skourski,[3] J. Wosnitza,[3,4] M. Farle,[2] and O. Gutfleisch[1]

[1]*Technische Universität Darmstadt, Institut für Materialwissenschaft, Alarich-Weiss-Straße 16, 64287 Darmstadt, Germany*

[2]*Fakultät für Physik und CENIDE, Universität Duisburg-Essen, 47057 Duisburg, Germany*

[3]*Dresden High Magnetic Field Laboratory (HLD-EMFL), Helmholtz-Zentrum Dresden-Rossendorf, 01328 Dresden, Germany*

[4]*Institut für Festkörperphysik, TU Dresden, 01062 Dresden, Germany*

(Received 16 December 2015; published 26 February 2016)

Large magnetocaloric effects can be obtained in Ni-Mn-based Heusler alloys due to the magnetostructural transition between martensite and austenite. This phase transformation proceeds via nucleation and growth. By direct measurements of the adiabatic temperature change ΔT_{ad} using different magnetic-field-sweeping rates from 0.01 up to 1500 $\mathrm{T\,s^{-1}}$, we study the dynamic behavior of the two Heusler compounds $Ni_{50}Mn_{35}In_{15}$ and $Ni_{45}Mn_{37}In_{13}Co_5$ transforming near room temperature. From these experiments, we conclude that the nucleation process is rather slow in contrast to the relatively fast movement of the phase boundary between martensite and austenite. This is a limiting factor for cooling concepts operating at frequencies beyond 100 Hz. However, the dynamic effects of the transition are negligible in field rates typically used in magnetic refrigeration. These findings are essential considering the suitability of Heusler compounds for energy-efficient solid-state cooling.

DOI: 10.1103/PhysRevApplied.5.024013

I. INTRODUCTION

Magnetocaloric cooling technology could be able to enter the refrigeration market in the near future when engineers and scientists manage to build machines working at a high operation frequency and performance with costs comparable to conventional devices [1,2]. For this purpose, the implementation of magnetocaloric materials with a first-order magnetostructural transition is needed. For instance, in La-Fe-Si- [3–7] or Fe_2P-type materials [8–10], the adiabatic temperature change ΔT_{ad} is comparable to the benchmark material Gd (second order) but the corresponding isothermal entropy change ΔS_T can be much larger. More heat can, therefore, be transferred from the cold to the hot side in every cooling cycle [11].

Both ΔT_{ad} and ΔS_T are essential in order to assess the suitability of the material. Most publications, however, consider only the isothermal entropy change which is usually derived indirectly using the Maxwell equation from magnetization isotherms [12]. Those measurements are typically done in isothermal or isofield conditions with small sweep rates of temperature or magnetic field.

Another approach is to determine ΔS_T by calorimetry in magnetic fields [13,14]. Usually electro- or superconducting magnets are used as the magnetic-field source. The latter results in a limitation of the field-application rate to approximately 1 $\mathrm{T\,min^{-1}}$. Both techniques operate under quasistatic conditions and are, therefore, very slow in comparison to the typical field rates in real applications.

There are only a few facilities around the world which allow the measurement of the adiabatic temperature change directly (the list makes no claim to completeness). In principle, four different possibilities to generate a magnetic-field change can be found: (a) sweeping the magnetic field of a superconducting or electromagnet [15,16], (b) introducing and extracting the sample from the magnetic-field source [17,18], (c) rotating of nested magnet assemblies in order to weaken or strengthen the magnetic field [19–21], and (d) creating magnetic-field pulses in a solenoid [22,23]. All of these techniques operate on very different time scales.

In this work, we selected two Heusler alloys with martensitic transitions near room temperature. The ternary and quaternary compounds Ni-Mn-In and Ni-Mn-In-Co are among the most interesting candidates in the Heusler family with first-order magnetostructural transitions in terms of their magnetocaloric properties [21]. The martensitic transformation between the low-temperature martensite and the high-temperature austenite phase manifests itself in an inverse magnetocaloric effect because the magnetization increases with temperature during the transition. As a consequence, the material cools when applying a magnetic field adiabatically.

This transition between martensite and austenite is driven by nucleation and growing of the "new" phase

*gottschall@fm.tu-darmstadt.de

[24–26]. We could show that large reversible temperature changes can be obtained in Ni-Mn-In-Co for minor loops of hysteresis with an incomplete transition [27]. The reason for this is the prevention of the energy-intensive nuclei formation in these minor hysteresis loops. Therefore, the magnetocaloric effect is mainly due to the movement of the boundary between martensite and austenite, which costs much less energy.

Recently, Ossmer *et al.* [28] investigated the kinetics of the martensitic transition in the elastocaloric material NiTi with *in situ* infrared thermography. By applying different strain rates, they could show that the manner of the phase conversion is strongly time dependent. In this paper, we transfer this approach to the first-order martensitic transformation of magnetocaloric Heusler compounds with a transition near room temperature by applying magnetic fields with various speeds. For this purpose, we compare direct measurements of the adiabatic temperature change ΔT_{ad} obtained in three different devices which cover magnetic-field-sweep rates as used in calorimetry of about 0.01 $\mathrm{T\,s^{-1}}$ up to high-frequency applications with field rates above 1000 $\mathrm{T\,s^{-1}}$.

II. EXPERIMENTAL DETAILS

Two samples with nominal compositions of $Ni_{50}Mn_{35}In_{15}$ and $Ni_{45}Mn_{37}In_{13}Co_5$ are prepared from high-purity elements by arc melting. The ingots are turned and remelted several times in order to assure chemical homogeneity. The compounds are then annealed at 900 °C for 24 h followed by water quenching. Magnetic measurements are performed in a commercial vibrating sample magnetometer from LakeShore. Direct measurements of the adiabatic temperature change ΔT_{ad} are carried out in three different devices with varying field-application rates in the discontinuous protocol (heating and cooling through the transition before each measurement).

(1) The slow measurements of ΔT_{ad} are performed inside a superconducting magnet [29,30]. The magnetic field changes with 0.66 $\mathrm{T\,min^{-1}}$. The thermocouple is placed in a drilled bore inside the sample. It is suspended and insulated by thin wires in a high-vacuum adiabatic calorimeter inside the bore of the magnet.

(2) The semifast measurement is carried out in a device with two nested Halbach magnets where the field can be varied between 0 and 1.93 T by rotating them in counter directions [31]. Therefore, the magnetic-field profile follows a sinusoidal shape with a starting field rate of 0.7 $\mathrm{T\,s^{-1}}$. A differential-type T thermocouple is glued to the sample with thermal-conductive epoxy.

(3) The adiabatic temperature-change measurements in pulsed fields up to 10 T are done in a solenoid [23]. The maximum field is applied in within 0.01 s, which compares to a field-sweep rate up to 1500 $\mathrm{T\,s^{-1}}$. A differential-type T thermocouple made of 25-μm-thin wires is glued between two plates of the sample with a thermal-conductive epoxy to determine the temperature change. The background signal of the thermocouple is obtained at low temperatures in the absence of any magnetocaloric effects in order to correct the measurement signal. In addition, a metrologically caused 50-Hz noise is removed subsequently. The magnetic field is measured with a pickup coil. Test measurements far from any magnetocaloric transition as well as experiments on different materials suggest that eddy current heating is negligible.

The absolute temperature measurement of the three devices is studied subsequently based on ΔT_{ad} experiments in the vicinity of the Curie temperature T_C^A of the austenite phase. In order to match the properties of the second-order transition around T_C^A, a correction of the starting temperatures of the pulsed-field measurements by +3 K is performed.

III. RESULTS AND DISCUSSION

Figures 1(a) and 1(b) show the magnetic properties of the two compounds under investigation. The magnetization as a function of temperature is measured in constant magnetic

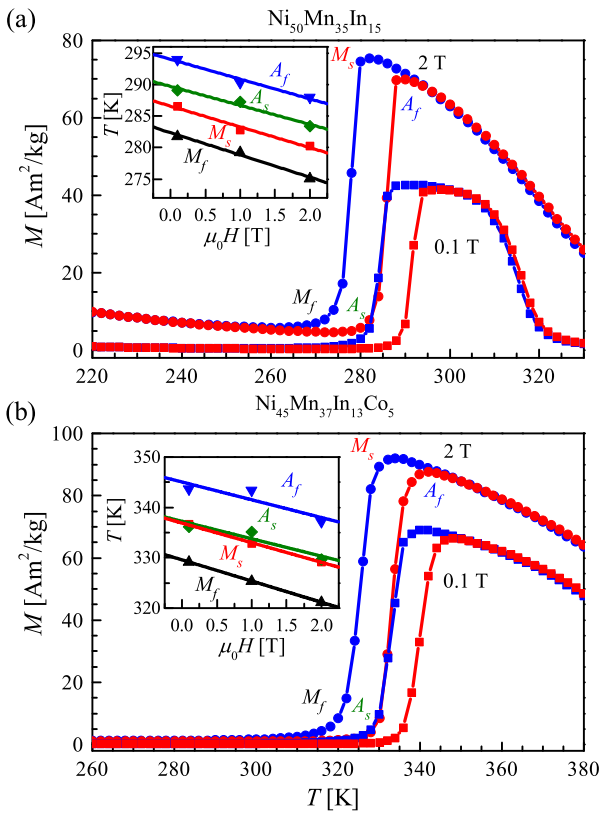

FIG. 1. Magnetization as a function of temperature obtained in 0.1 and 2 T of (a) Ni-Mn-In and (b) Ni-Mn-In-Co. The inset shows the magnetic phase diagram (martensite start M_s, martensite finish M_f, austenite start A_s, austenite finish A_f).

fields of 0.1 and 2 T. The strong first-order character of the transition is visible around 280 K for the Heusler material without Co and 330 K for the one with Co. The samples undergo an inverse magnetocaloric transition and, therefore, the magnetization rises due to the transformation from the low-temperature martensite to the high-temperature austenite phase. The transition shows a thermal hysteresis of about 8 K in both materials. For Ni-Mn-In, the magnetization drops down above room temperature due to the Curie temperature $T_C^A = 314$ K of the austenite. This purely magnetic transition is of a conventional type. The partial substitution of Ni by Co increases the T_C^A up to around 400 K [see Fig. 1(b)]. From the isofield measurements the shift of the transition temperature in magnetic fields can be determined by plotting and linear fitting [inset of Figs. 1(a) and 1(b)] of the temperature's martensite start M_s, martensite finish M_f, austenite start A_s, and austenite finish A_f, which describe the transition shape and hysteresis. It is found that the transition is shifted to lower temperatures by about $-3.2\ \mathrm{K\,T^{-1}}$ for the Co-free and $-3.7\ \mathrm{K\,T^{-1}}$ for the Co-containing sample in magnetic fields. These values will be important in the following investigation of the adiabatic temperature change.

In the next paragraphs the temperature evolution of the samples in the three devices will be presented beginning with the slow technique (superconducting magnet).

A. Superconducting magnet setup

For this setup, the temperature change under magnetization and demagnetization is shown in Fig. 2 for $Ni_{50}Mn_{35}In_{15}$. The magnetic-field profile is illustrated in dashed lines in the shape of a trapezoidal function. The ramping time is about 400 s to reach the maximum of 5 T. It can be seen that the sample cools down immediately when applying the magnetic field. Before that, the temperature is stabilized at about 284 K. Because of imperfect adiabaticity and the long measurement time, the sample temperature drifts back to the initial temperature with about $0.16\ \mathrm{K\,min^{-1}}$. This process is visible in Fig. 2.

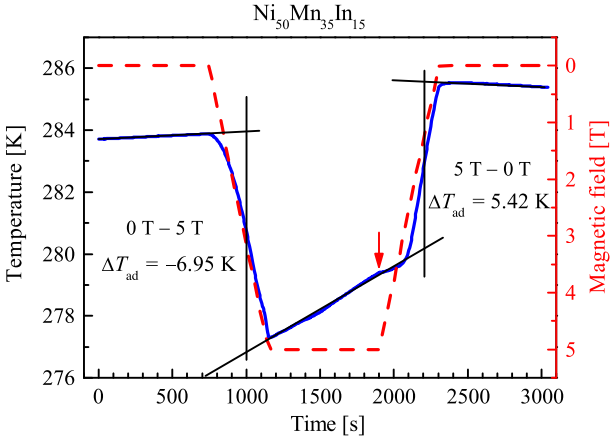

FIG. 2. Temperature evolution of the sample in a slow field-application rate (superconducting magnet).

The real ΔT_{ad} can be approximated by describing the curve before and after the measurement with linear fits leading to a value of -6.95 K for a magnetic-field change of 5 T. In order to determine the temperature drift a certain waiting time is needed. Since the drift in temperature is significant, the demagnetization is no longer comparable with the magnetization process. Nevertheless, a large reversible temperature change is observed, meaning that the thermal hysteresis can be overcome. The small hump around 1900 s (indicated by an arrow in Fig. 2) when the magnetic field is decreasing again is no anomaly. It is due to the conventional magnetocaloric effect of the high-temperature austenite phase which will be considered in detail later.

B. Halbach magnet setup

Figure 3 shows the cooling and heating curves of the sample when the magnetic field is applied in a semifast way in the Halbach setup. The two nested Halbach magnets generate a sinusoidal magnetic-field change in within approximately 18 s (field rate of $0.7\ \mathrm{T\,s^{-1}}$ in the beginning of the experiment). This is about 60 times faster than the measurement in the superconducting magnet, but, nevertheless, the sample temperature perfectly follows the magnetic field. For these Heusler alloys the magnetic-field

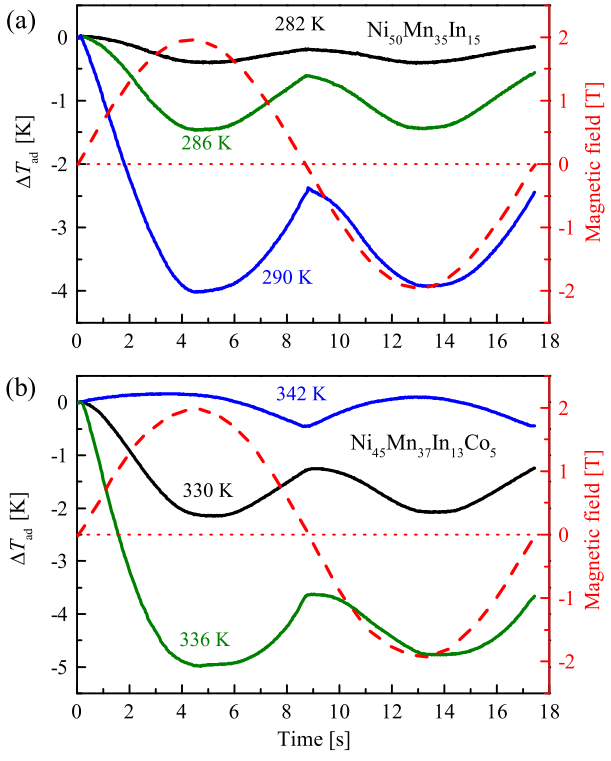

FIG. 3. Temperature evolution of (a) $Ni_{50}Mn_{35}In_{15}$ and (b) $Ni_{45}Mn_{37}In_{13}Co_5$ for a semifast field-application rate (Halbach magnet).

direction is not important, only the value is of significance. For this reason, one magnet rotation allows the measuring of two magnetization and demagnetization cycles. The maximum ΔT_{ad} in 1.93 T, which is about −4 K for Ni-Mn-In and −5 K for Ni-Mn-In-Co, can be observed at starting temperatures of 290 and 336 K, respectively. When decreasing the magnetic field to zero again, the temperature does not reach the initial state. This irreversibility is due to the significant thermal hysteresis of about 8 K in the two compounds.

A reversible effect is visible in the second field-application cycle amounting to 1.5 K in Fig. 3(a) which is caused by the minor loop behavior (see Ref. [27]). The magnitude of ΔT_{ad} which can be observed in the first and second magnetic-field application strongly depends on the starting temperature. At lower temperature [e.g., at 286 K in Fig. 3(a)] the sample transforms more and more reversibly but the overall effect decreases as well. Above the transition the conventional magnetocaloric effect of the austenite phase becomes dominant as illustrated by the data taken at 342 K in Fig. 3(b). This results in a positive temperature change which reaches its maximum at the austenitic Curie temperature.

C. Pulsed-field-magnet setup

In Fig. 4, the temperature evolution of the two samples exposed to pulsed magnetic fields is plotted for selected starting temperatures (the temporal field profiles are shown again by dashed lines). In this setup a magnetic field of 10 T is reached in approximately 13 ms, whereas the decreasing branch is considerably longer. Despite the high field-sweep rate (up to 1500 T s^{-1}), the thermocouple can follow the sample-temperature change without time delay, being evidence for the reliability of the measurement. The largest ΔT_{ad} of −13 K is observed in $Ni_{45}Mn_{37}In_{13}Co_5$ [Fig. 4(b)] when the sample is heated to 328.5 K before the magnetic-field pulse. It can be seen that the temperature does not return to the initial value because of a thermal hysteresis. This is different, for instance, in the experiment at 323.2 K. A clear interpretation of the ongoing processes is rather difficult when plotting ΔT_{ad} vs time. Especially, the nonmonotonic behavior around the maximum magnetic field [Fig. 4(a)] seems puzzling. A better understanding is possible when the adiabatic temperature change is monitored as a function of the magnetic field instead, which will be discussed in the following.

D. Magnetic-field dependence

Measurements of the adiabatic temperature change are performed in three different pulsed magnetic fields of 2, 5, and 10 T in order to compare the obtained results with those determined by the superconducting magnet and Halbach setup. The conventional second-order transition of the ferromagnetic austenite phase around the Curie temperature T_C^A is a purely magnetic transition. No thermal-hysteresis

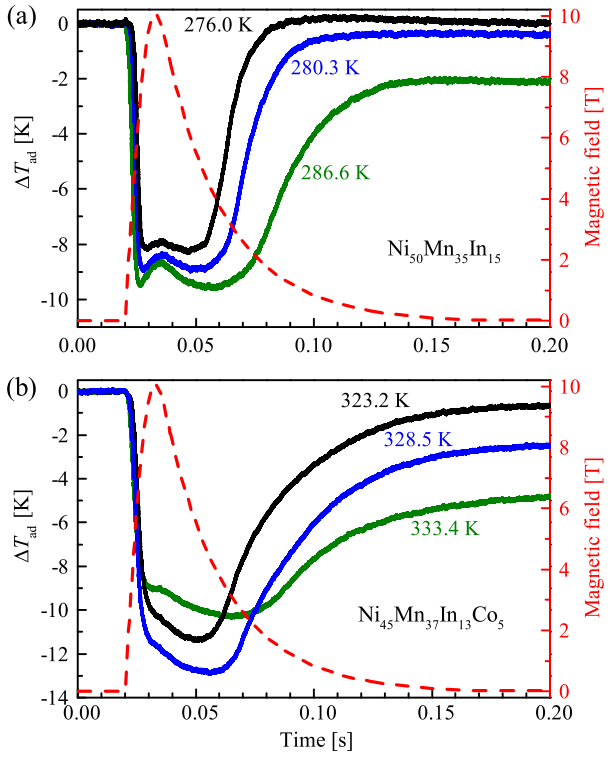

FIG. 4. Temperature evolution of (a) the Co-free and (b) the Co-containing sample for a fast field-application rate (pulsed-field solenoid).

effect is associated with this ferromagnetic-to-paramagnetic transition, for instance, alike for the benchmark material Gd. Therefore, ΔT_{ad} for increasing and decreasing field must coincide for a second-order transition. The obtained ΔT_{ad} as a function of the magnetic field for $Ni_{50}Mn_{35}In_{15}$ at about 317 K is shown in the inset of Fig. 5(a). If the thermocouple response during the pulse would be too slow, an artificial hysteresis loop would appear. Since this is not the case, the temperature determination is highly reliable, even for the fast field-sweep rates used here.

The characteristics change drastically when measuring the response of the first-order phase transition. In this case, the thermal hysteresis of the martensitic transition leads to a hysteretic ΔT_{ad} dependence as shown in Fig. 5. The results for the three different pulsed magnetic fields are compared for a single starting temperature. The measurements are performed in the discontinuous protocol, meaning that the sample is heated to the austenitic and cooled to the martensitic state between the measurements in order to erase the history of the material [21].

The starting temperature of 286.6 K is rather close to the first-order transition but in zero field most of the sample is still in the martensite state, as can be seen from the magnetization data [Fig. 1(a)]. Looking at the 10-T curve [Fig. 5(b)], the specimen starts to cool down slightly when applying the magnetic field. When passing 3 T, the cooling accelerates and finally saturates around 6 T. At this point

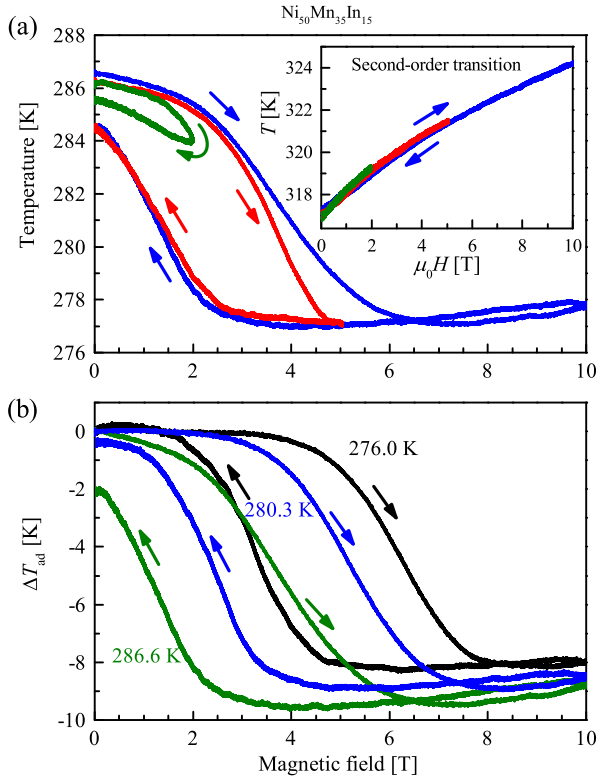

FIG. 5. (a) Field dependence of the absolute temperature of the Co-free sample in different pulsed magnetic fields and (b) ΔT_{ad} for different starting temperatures. The inset in (a) shows the results close to the second-order ferromagnetic phase transition at 314 K.

the sample is completely transformed into the austenite and because of the proximity to the Curie temperature the sample heats up due to the conventional magnetocaloric effect when increasing the magnetic field further. For the demagnetization, first the temperature changes slightly, following the conventional magnetocaloric behavior at this condition. Below about 4 T, the transition into the martensite state starts and the sample heats up but cannot reach the starting temperature due to the width of the thermal hysteresis. It is possible to overcome the large thermal hysteresis when starting the process at lower initial temperatures as shown in Fig. 5(b). For instance, at 280.3 K, the transition is nearly reversible for the 10-T pulse, but the lower the starting temperature is, the higher magnetic fields are needed to complete the transition. From this context, it is obvious that the nonmonotonic behavior observed in Fig. 4(a) in magnetic fields exceeding 5 T is due to the conventional magnetocaloric effect of the austenite.

For the 5-T pulse [Fig. 5(a)] the transition also can be fully completed. Interestingly, the material cools faster with increasing field than in the case of 10 T, however, the demagnetization curve behaves very similarly. We relate this effect to different magnetic-field rates in the experiments and to the time dependence of the martensitic transition, as it will be discussed later.

Also the 2-T pulse is plotted in Fig. 5(a). The martensite-to-austenite transition starts even earlier than in the case of the 5-T pulse. The maximum field for this measurement is not sufficient to completely transform the material and, therefore, the demagnetization branch in this hysteresis loop is different from the curves with complete transitions [27,32].

The temporal magnetic-field profiles are shown in Fig. 6(a). The time needed to reach the maximum field is the same for all three applied magnetic fields. As a consequence, the field-sweep rates depend on the maximum magnetic field. In order to illustrate this, the sweep rate $\mu_0(dH/dt)$ is plotted as a function of magnetic field in Fig. 6(b) for the 2-, 5-, and 10-T pulses. When applying the 10-T pulse the field rate exceeds 1500 $\mathrm{T\,s^{-1}}$. By multiplying this value with the shift of the transition temperature in magnetic fields as shown in Fig. 1, the field rate can be compared with a respective cooling or heating condition the sample would be subject to. For the compound $Ni_{50}Mn_{35}In_{15}$, this related cooling rate $\beta = (dH/dt)(dT_t/dH)$ is about 300 000 $\mathrm{K\,min^{-1}}$ at its maximum which illustrates the extreme conditions in the measurements.

For 5 and 2 T, the rates are smaller accordingly. The important feature of the magnetic-field changes becomes obvious for the negative rates [Fig. 6(b)]. The magnetic-field-sweep rates decrease linearly to zero. This plot can explain the behavior observed in Fig. 5(a) for the 5 and 10 T curve. The field-sweep rate during the magnetization process differs a lot, but it is largely field-pulse independent

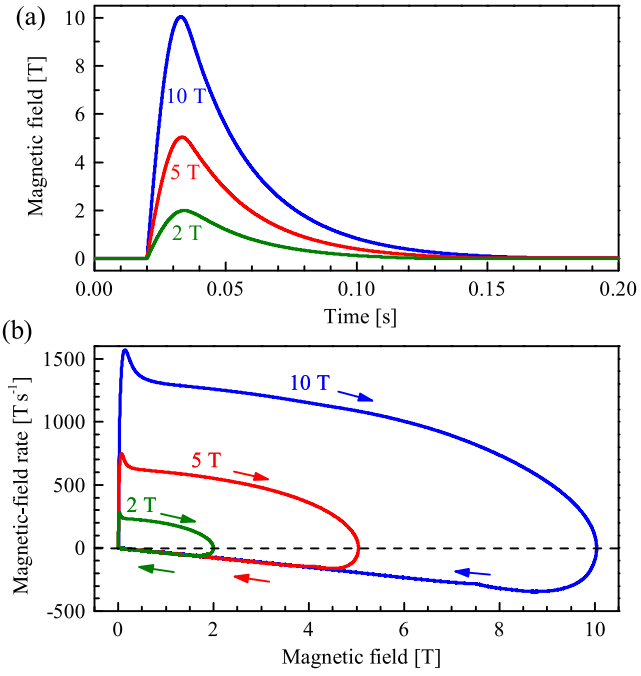

FIG. 6. (a) Pulsed magnetic-field profiles as a function of time. (b) Field-sweep rates vs magnetic field.

for the demagnetization process. Consequently, the speed of the backward transformation in the two experiments is comparable. This means that the differences in the magnetization branches between the 5- and 10-T pulse must be due to kinetic reasons of the martensitic transition.

Similar effects as discussed for $Ni_{50}Mn_{35}In_{15}$ are also observed for $Ni_{45}Mn_{37}In_{13}Co_5$ (not shown), confirming time-dependent effects of the martensitic transition for the Co-containing system as well.

E. Comparison of the magnetic-field dependences

In the following, the focus will be on the comparison of the results obtained by the use of the three experimental techniques. It should be mentioned that for a reasonable comparison the starting temperatures in all three devices must be as close as possible, at least to within 0.5 K. The results will be exemplarily discussed for the Co-free compound. For Ni-Mn-In, 5- and 2-T cooling curves for one magnetic-field cycle are plotted in Fig. 7.

ΔT_{ad} measured for a 5-T pulse behaves similarly to the one in Fig. 5(a), which is discussed in detail already. The cooling behavior of the sample for the low sweep rate using the superconducting magnet is plotted in Fig. 7 as well. Because of the pronounced temperature drift during the measurement (see Fig. 2), there is a jump at the maximum field and, therefore, the heating curve (dotted line) is only of limited relevance. On the other hand, the small ΔT_{ad} loop which is obtained in the Halbach setup shows the typical minor-loop behavior leading to a relatively large reversible magnetocaloric effect [27].

There is, however, an important observation in Fig. 7. It turns out that the slope in the midregion of the cooling curves is the same for all three techniques and, therefore, independent of the field-sweep rate. The related cooling rates are 2.3 $K\,min^{-1}$ for the superconducting magnet, 135 $K\,min^{-1}$ for the Halbach magnet, and about 300 000 $K\,min^{-1}$ in pulsed magnetic fields.

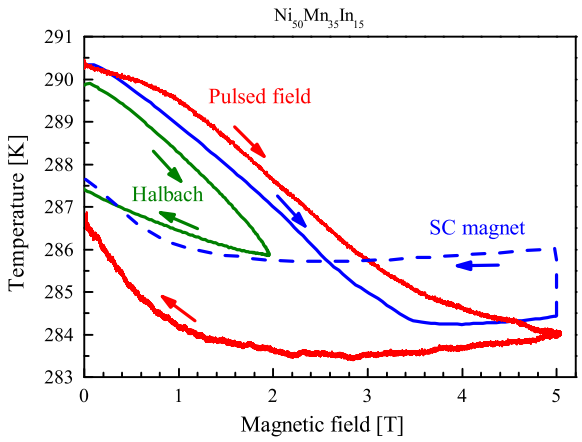

FIG. 7. Comparison of ΔT_{ad} as a function of magnetic field obtained by use of the three experimental techniques.

However, there are some differences between the slow and the fast measurement. For the superconducting magnet the sample cools strongly immediately when switching on the field, whereas for pulsed fields the sample needs more time to reach the maximum cooling rate. The same feature is observed (Fig. 5) when comparing pulsed-field measurements with different field-sweep rates. Around 3.5 T the martensitic transition is completed in the superconducting magnet but the total adiabatic temperature change of the pulsed-field measurement is not reached up to 5 T. This difference of about 0.5 K is due to the unavoidable nonadiabatic condition during the 400-s measurement time in the superconducting magnet.

Our obtained results of the adiabatic temperature change in different magnetic-field-sweep rates are consistent with recent findings in the literature. Xu *et al.* [33] performed magnetization measurements in pulsed magnetic fields on a similar Heusler compound and showed that the hysteresis increases with faster field sweeping. The first-order martensitic transition in these Heusler compounds is driven by the nucleation and growth mechanisms of martensite and austenite. Based on the finding that the maximum slope of ΔT_{ad} is independent of the field-sweep rate, at least up to 750 $T\,s^{-1}$, it seems reasonable to conclude that the phase-boundary movement is a rather fast process. In contrast, it is apparent from Figs. 5 and 7 that it is more and more difficult to initiate the martensitic transformation with fast field-sweep rates. It seems that the nucleation process of the new phase requires a slightly longer time than the simple phase-boundary movement. Therefore, the nucleation of austenite is delayed in the fast pulsed-field experiments. Consequently, the ΔT_{ad} curve falls behind the slow and semifast results in Fig. 7 between 0 and 1 T.

Despite the very different time scales in the three setups it can be concluded that the martensitic transition of the investigated Heusler compounds with transformation near room temperature is always fast enough to follow the magnetic field. It can be concluded that the Heusler compounds can operate at realistic frequencies of a typical active-magnetic-regenerator (AMR) device up to 10 Hz which makes them excellent candidates to be utilized in applications. On the other hand, for concepts operating at frequencies of 100 Hz and more [34], the kinetics of the first-order transition comes into play and must be considered.

F. Maximum adiabatic temperature change

It remains to compare the adiabatic temperature change in the respective maximum magnetic fields for the three experimental techniques plotted in Fig. 8(a) for $Ni_{50}Mn_{35}In_{15}$ and 8(b) for $Ni_{45}Mn_{37}In_{13}Co_5$. In the small magnetic-field changes of 1.93 T in the Halbach setup the transition cannot be completed. Therefore, the ΔT_{ad} curve has a peak shape. However, magnetic-field strengths of 5 T are sufficient to fully transform the material and a plateau of

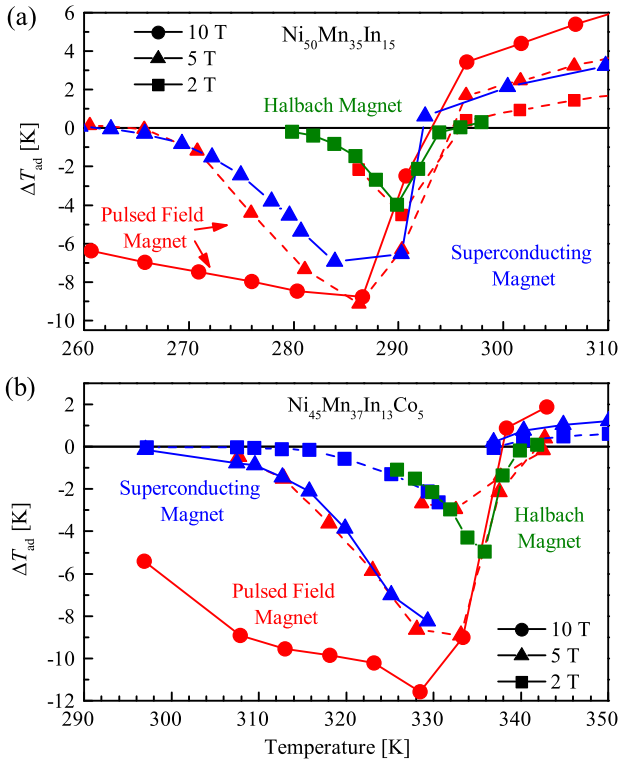

FIG. 8. Adiabatic temperature change of (a) $Ni_{50}Mn_{35}In_{15}$ and (b) $Ni_{45}Mn_{37}In_{13}Co_5$ at the maximum field for the three different experimental techniques.

the temperature change is visible leading to values of −9 K for the Co-free and −11.5 K for the Co-containing sample. At higher temperatures, the temperature change becomes positive due to the conventional magnetocaloric effect caused by the ferromagnetic transition with Curie temperatures at 314 and 400 K, respectively. This overlapping of the first- and second-order transition is the main reason why the Clausius-Clapeyron equation predicts slightly higher ΔT_{ad} values of about −12.2 K for $Ni_{50}Mn_{35}In_{15}$ and −14.2 K for $Ni_{45}Mn_{37}In_{13}Co_5$.

Using faster magnetic-field changes further extends the ΔT_{ad} plateau to lower temperatures and the access to higher significant reversible magnetocaloric effects over a wide temperature window. This behavior is as expected since the transition can be induced already at lower temperatures when the magnetic-field strength is higher.

IV. CONCLUSION

In summary, we compare direct measurements of the adiabatic temperature change ΔT_{ad} of the ternary and quaternary Heusler compounds $Ni_{50}Mn_{35}In_{15}$ and $Ni_{45}Mn_{37}In_{13}Co_5$ with transitions near room temperature. Three different setups are used spanning over 5 orders of field-sweep rates, from 0.01 up to 1500 $T\,s^{-1}$.

Large magnetocaloric effects up to −11.5 K are found in pulsed fields of 10 T. In the superconducting magnet the samples could also be transformed completely at 5 T. The Halbach setup, where only 1.93 T can be achieved and the transition cannot be completed, allows us to observe an initial and reversible temperature change of −4.0 and −1.5 K, respectively.

From the adiabatic temperature change ΔT_{ad} as a function of the magnetic field we could demonstrate that the martensitic transition is indeed time dependent. It turned out that the nucleation process and the phase-boundary movement which are both responsible for the transformation, act on different time scales. The movement of the phase boundary is rather fast. For this reason, the maximum slope of ΔT_{ad} as a function of field, being related to the transformation rate, is similar in all three devices. In contrast to that, the initialization of the transition which is mainly due to nucleation processes is hindered when the field-sweep rate becomes faster. This is a limiting factor which needs to be considered for magnetocaloric applications with cycling frequencies beyond 100 Hz. But for typical AMR-device frequencies up to 10 Hz we could show that Heusler compounds are useful refrigerants for solid-state magnetic-cooling technology.

ACKNOWLEDGMENTS

This work was supported by DFG (Grant No. SPP 1599) and by HLD at HZDR, member of the European Magnetic Field Laboratory (EMFL).

[1] B. Monfared, R. Furberg, and B. Palm, Magnetic vs. vapor-compression household refrigerators: A preliminary comparative life cycle assessment, Int. J. Refrig. **42**, 69 (2014).
[2] A. Kitanovski, J. Tušek, U. Tomc, U. Plaznik, M. Ozbolt, and A. Poredoš, *Magnetocaloric Energy Conversion: From Theory to Applications*, Green Energy and Technology (Springer International Publishing, 2014).
[3] S. Fujieda, A. Fujita, and K. Fukamichi, Large magnetocaloric effect in $La(Fe_xSi_{1-x})_{13}$ itinerant-electron metamagnetic compounds, Appl. Phys. Lett. **81**, 1276 (2002).
[4] O. Gutfleisch, A. Yan, and K.-H. Müller, Large magnetocaloric effect in melt-spun $LaFe_{13-x}Si_x$, J. Appl. Phys. **97**, 10M305 (2005).
[5] K. G. Sandeman, Magnetocaloric materials: The search for new systems, Scr. Mater. **67**, 566 (2012).
[6] J. Liu, J. D. Moore, K. P. Skokov, M. Krautz, K. Löwe, A. Barcza, M. Katter, and O. Gutfleisch, Exploring $La(Fe, Si)_{13}$-based magnetic refrigerants towards application, Scr. Mater. **67**, 584 (2012).
[7] I. A. Radulov, K. P. Skokov, D. Yu. Karpenkov, T. Gottschall, and O. Gutfleisch, On the preparation of $La(Fe, Mn, Si)_{13}H_x$ polymer-composites with optimized magnetocaloric properties, J. Magn. Magn. Mater. **396**, 228 (2015).
[8] E. Brück, Developments in magnetocaloric refrigeration, J. Phys. D **38**, R381 (2005).
[9] A. Yan, K.-H. Müller, L. Schultz, and O. Gutfleisch, Magnetic entropy change in melt-spun MnFePGe (invited), J. Appl. Phys. **99**, 08K903 (2006).

[10] F. Guillou, H. Yibole, G. Porcari, L. Zhang, N. H. van Dijk, and E. Brück, Magnetocaloric effect, cyclability and coefficient of refrigerant performance in the MnFe(P, Si, B) system, J. Appl. Phys. **116**, 063903 (2014).

[11] K. P. Skokov, A. Yu. Karpenkov, D. Yu. Karpenkov, and O. Gutfleisch, The maximal cooling power of magnetic and thermoelectric refrigerators with $La(FeCoSi)_{13}$ alloys, J. Appl. Phys. **113**, 17A945 (2013).

[12] A. Smith, C. R. H. Bahl, R. Björk, K. Engelbrecht, K. K. Nielsen, and N. Pryds, Materials challenges for high performance magnetocaloric refrigeration devices, Adv. Energy Mater. **2**, 1288 (2012).

[13] E. Palacios, G. F. Wang, R. Burriel, V. Provenzano, and R. D. Shull, Direct measurement of the magnetocaloric effect in $Gd_5Si_2Ge_{1.9}Ga_{0.1}$, J. Phys. Conf. Ser. **200**, 092011 (2010).

[14] V. Basso, M. Küpferling, C. P. Sasso, and L. Giudici, A Peltier cell calorimeter for the direct measurement of the isothermal entropy change in magnetic materials, Rev. Sci. Instrum. **79**, 063907 (2008).

[15] S. Aksoy, T. Krenke, M. Acet, E. F. Wassermann, X. Moya, L. Manosa, and A. Planes, Tailoring magnetic and magnetocaloric properties of martensitic transitions in ferromagnetic Heusler alloys, Appl. Phys. Lett. **91**, 241916 (2007).

[16] L. Tocado, E. Palacios, and R. Burriel, Direct measurement of the magnetocaloric effect in $Tb_5Si_2Ge_2$, J. Magn. Magn. Mater. **290–291**, 719 (2005).

[17] M. Katter, V. Zellmann, G. W. Reppel, and K. Uestuener, Magnetocaloric properties of $La(Fe, Co, Si)_{13}$ bulk material prepared by powder metallurgy, IEEE Trans. Magn. **44**, 3044 (2008).

[18] H. Yibole, F. Guillou, L. Zhang, N. H. van Dijk, and E. Brück, Direct measurement of the magnetocaloric effect in $MnFe(P, X)$ ($X =$ As, Ge, Si) materials, J. Phys. D **47**, 075002 (2014).

[19] A. P. Kazakov, V. N. Prudnikov, A. B. Granovsky, A. P. Zhukov, J. Gonzalez, I. Dubenko, A. K. Pathak, S. Stadler, and N. Ali, Direct measurements of field-induced adiabatic temperature changes near compound phase transitions in Ni-Mn-In based Heusler alloys, Appl. Phys. Lett. **98**, 131911 (2011).

[20] V. V. Khovaylo, K. P. Skokov, O. Gutfleisch, H. Miki, R. Kainuma, and T. Kanomata, Reversibility and irreversibility of magnetocaloric effect in a metamagnetic shape memory alloy under cyclic action of a magnetic field, Appl. Phys. Lett. **97**, 052503 (2010).

[21] J. Liu, T. Gottschall, K. P. Skokov, J. D. Moore, and O. Gutfleisch, Giant magnetocaloric effect driven by structural transitions, Nat. Mater. **11**, 620 (2012).

[22] T. Kihara, X. Xu, W. Ito, R. Kainuma, and M. Tokunaga, Direct measurements of inverse magnetocaloric effects in metamagnetic shape-memory alloy NiCoMnIn, Phys. Rev. B **90**, 214409 (2014).

[23] M. Ghorbani Zavareh, C. Salazar Mejia, A. K. Nayak, Y. Skourski, J. Wosnitza, C. Felser, and M. Nicklas, Direct measurements of the magnetocaloric effect in pulsed magnetic fields: The example of the Heusler alloy $Ni_{50}Mn_{35}In_{15}$, Appl. Phys. Lett. **106**, 071904 (2015).

[24] T. Gottschall, K. P. Skokov, R. Burriel, and O. Gutfleisch, On the $S(T)$ diagram of magnetocaloric materials with first-order transition: Kinetic and cyclic effects of Heusler alloys, Acta Mater. **107**, 1 (2016).

[25] A. Banerjee, P. Chaddah, S. Dash, Kranti Kumar, Archana Lakhani, X. Chen, and R. V. Ramanujan, History-dependent nucleation and growth of the martensitic phase in the magnetic shape memory alloy $Ni_{45}Co_5Mn_{38}Sn_{12}$, Phys. Rev. B **84**, 214420 (2011).

[26] M. K. Chattopadhyay, K. Morrison, A. Dupas, V. K. Sharma, L. S. Sharath Chandra, L. F. Cohen, and S. B. Roy, Study of the dynamical features of the austenite-martensite phase transition in the $Ni_{50}(Mn, 1\%Fe)_{34}In_{16}$ alloy using scanning Hall probe imaging, J. Appl. Phys. **111**, 053908 (2012).

[27] T. Gottschall, K. P. Skokov, B. Frincu, and O. Gutfleisch, Large reversible magnetocaloric effect in Ni-Mn-In-Co, Appl. Phys. Lett. **106**, 021901 (2015).

[28] H. Ossmer, C. Chluba, M. Gueltig, E. Quandt, and M. Kohl, Local Evolution of the Elastocaloric Effect in TiNi-Based Films, Shape Mem. Superelasticity **1**, 142 (2015).

[29] Ö. Cakir and M. Acet, Reversibility in the inverse magnetocaloric effect in Mn_3GaC studied by direct adiabatic temperature-change measurements, Appl. Phys. Lett. **100**, 202404 (2012).

[30] F. Scheibel, T. Gottschall, K. Skokov, O. Gutfleisch, M. Ghorbani-Zavareh, Y. Skourski, J. Wosnitza, Ö. Cakir, M. Farle, and M. Acet, Dependence of the inverse magnetocaloric effect on the field-change rate in Mn_3GaC and its relationship to the kinetics of the phase transition, J. Appl. Phys. **117**, 233902 (2015).

[31] K. P. Skokov, D. Yu. Karpenkov, M. D. Kuzmin, I. A. Radulov, T. Gottschall, B. Kaeswurm, M. Fries, and O. Gutfleisch, Heat exchangers made of polymer-bonded $La(Fe, Si)_{13}$, J. Appl. Phys. **115**, 17A941 (2014).

[32] I. Titov, M. Acet, M. Farle, D. Gonzalez-Alonso, L. Manosa, A. Planes, and T. Krenke, Hysteresis effects in the inverse magnetocaloric effect in martensitic Ni-Mn-In and Ni-Mn-Sn, J. Appl. Phys. **112**, 073914 (2012).

[33] X. Xu, T. Kihara, M. Tokunaga, A. Matsuo, W. Ito, R. Y. Umetsu, K. Kindo, and R. Kainuma, Magnetic field hysteresis under various sweeping rates for Ni-Co-Mn-In metamagnetic shape memory alloys, Appl. Phys. Lett. **103**, 122406 (2013).

[34] A. Kitanovski and P. W. Egolf, Innovative ideas for future research on magnetocaloric technologies, Int. J. Refrig. **33**, 449 (2010).